Rheologic controls on inter-rifting deformation of the Northern Volcanic Zone, Iceland

Rikke Pedersen [a,*], Freysteinn Sigmundsson [a], Timothy Masterlark [b]

[a] Nordic Volcanological Center, Institute of Earth Sciences, University of Iceland, Reykjavik, Iceland
[b] Department of Geological Sciences, University of Alabama, Tuscaloosa, USA

ARTICLE INFO

ABSTRACT

Extensional rifts are characterized by significant lateral variations in crustal rheology as lithospheric material cools and advects away from the rift axes. Nevertheless, most models used for modeling of crustal movements consist of horizontal layers with uniform properties. This paper explores the role spatial variation of rheological properties play, in modifying the style of surface deformation at rifts, by comparing finite element model predictions to inferred inter-rifting surface deformation in Iceland's Northern Volcanic Zone. Crustal deformation has been observed by satellite radar interferometry (InSAR) and GPS measurements. Extension is observed across the entire northern rift zone, whereas subsidence occurs in two distinct areas, corresponding to mapped fissure swarms, where major rifting took place in 1975–1984 and 1874–1876, respectively. Our models indicate that the observed inter-rifting plate spreading deformation field is controlled by rheological variations within the *en echelon* arrangement of fissure segments, and that a central ridge axes model does not apply. Uniform stretching across a plate boundary zone, where fissure swarms are weaker than the surrounding crust, and reflect the surface expression of the rift, reproduces the characteristics of the deformation field. The most realistic fissure swarm structure consists of a wedge of weak elastic material on top of a ridge, where viscoelastic material locally reaches to a shallow depth.

© 2009 Elsevier B.V. All rights reserved.

1. Introduction

The processes responsible for plate motions have been extensively studied since the general acceptance of the theory of plate tectonics in the late 1960s (e.g. Dietz, 1961; Wilson, 1965; Morgan, 1968; Kearey and Vine, 1990, and references therein). Recent advances in space geodetic methods have provided an opportunity for major improvements in detailed characterization, analysis and modeling of physical processes within the Earth, which cause measurable deformation on the Earth's surface (Massonnet and Feigl, 1998). So far, the vast majority of detailed surface deformation studies at plate boundaries have been conducted at converging margins as diverging margins are only accessible above sea level at a few places around the world, such as in Iceland (mature ridge) (e.g. Heki et al., 1993; Jónsson et al., 1997; LaFemina et al., 2005; Árnadóttir et al., 2006) and in the Afar region in eastern Africa (nascent ridge) (e.g. Ruegg et al., 1993; Cattin et al., 2005; Wright et al., 2006; Vigny et al., 2007).

Typical plate spreading models simulating measured crustal deformation assume horizontal layers of constant thickness and rheology (e.g. Heki et al., 1993; Jónsson et al., 1997; LaFemina et al., 2005). Considerable improvements of these models may be attained by taking into account 2D, 3D or even transient variations in the

rheological characteristics of the lithospheric and asthenospheric layers (Masterlark et al., 2001; Cattin et al., 2005), affected by the plate spreading process. Such advanced models can provide more realistic Earth deformation simulations, hence may be more reliable as to represent a plate spreading scenario. A fundamental question regarding plate spreading models is what controls the diverging plates and their deformation on a scale of hundreds of km along axis, where a central spreading axis may form a segmented *en echelon* pattern of volcanic systems at the surface. Do these segments connect in the subsurface to form a large central rift axis, which controls the process, or do individual fissure swarms, making up the plate spreading zone in an *en echelon* pattern, play a major role? In order to differentiate between such scenarios, we need to investigate the effect that variations in rheology of lithospheric layers (e.g. Heki et al., 1993; Cattin et al., 2005) as well as distinct layer geometries, may have on surface deformation.

The motivation of our study originates from measurements of three dimensional surface deformation in the Northern Volcanic Zone (NVZ), Iceland, where vertical and horizontal deformation components are observed to work on different length scales. Our observations include a spreading segment in an inter-rifting phase showing horizontal strain accumulation over a much wider area than the associated vertical deformation. Previous models of plate spreading environments were designed mainly to predict GPS measurements of horizontal deformation, as the uncertainties of vertical GPS measurements are typically an

order of magnitude greater than uncertainties of corresponding horizontal components (Völksen, 2000). Furthermore, the signal to noise ratio, is poorer for the vertical than the horizontal component, as the vertical signal is considerably smaller (mm/yr) than the horizontal (cm/yr). As diverging plate boundaries are characterized by highly fractured crust, vertical offsets in deformation data may previously have been attributed to slight adjustments of preexisting weaknesses.

Interferometric synthetic aperture radar (InSAR) provides a measurement technique capable of detecting the subtle vertical adjustments of the crust in periods dominated by inter-rifting deformation. A series of InSAR images covering the NVZ reveal subtle, but persistent, subsidence confined within approximately 20 km wide fissure swarms, corresponding closely to parts of a mapped sub-segment of the plate boundary, whereas GPS measurements of horizontal deformation associated with plate spreading show a signal distributed over an almost 100 km wide plate boundary zone (Árnadóttir et al., in press). Gradual and coherent deformation signals within the mapped fissure swarms suggest variations in rheologic properties, rather than normal faulting, for which the deformation signal would be more localized.

In this study, we test a hypothesis that the observed apparent decoupling of horizontal and vertical deformation components may be attributed to variations in rheology and geometry of the underlying lithospheric layers. We use finite element models (FEM) to calculate 2D surface deformation patterns for inter-rifting periods resulting from a number of possible plate boundary scenarios, in order to deduce how the crustal structure influences the resulting surface deformation. We then use the results from the 2D models to guide the design and construction of relatively simple 3D models simulating plate spreading in the NVZ, to investigate whether plate spreading deformation is controlled by a central subsurface ridge or by individual fissure segments. We finally evaluate the 3D model predictions against deformation data from the plate-spreading segment in North Iceland, collected over a period believed to be representative of inter-rifting deformation.

2. The Northern Volcanic Zone

Our study area is the NVZ in Iceland, which forms a part of the Mid-Atlantic spreading ridge (Fig. 1). In Iceland, the mid-ocean ridge is exposed above sea level, as the interaction between a hotspot and the diverging plates creates an excess production of mantle melts, lifting the seafloor over a wide region (e.g., Ito et al., 1999, 2003). The source of the hotspot is generally accepted to be a deep mantle plume with excessive mantle upwelling (Sigmundsson, 2006), although alternative ideas exist relating the excess magmatism to melting of mantle entrained slabs of fusible, recycled ocean-crust material (Foulger, 2006).

2.1. Tectonic setting and historic volcanic activity

Plate spreading within Iceland is focused in an array of rift zones such as the NVZ (Fig. 1). In Iceland rift zones are temporally unstable structures and jumps occur at 5–10 Myr intervals, due to the relative drift between the location of the mantle plume and the spreading axis (Saemundsson, 1986; Einarsson, 1991). The NVZ has only been the main zone of spreading in the north for the past 6–7 Myr. Oblique extension (the direction of spreading is oblique to the regional trend of the deformation zone) characterizes the NVZ (Fig. 1). It has been divided into five *en echelon* spreading segments, each having a fissure swarm and an associated central volcano that is the focus of volcanic production and an area of high-temperature geothermal activity (Saemundsson, 1979; Einarsson and Sæmundsson, 1987). Caldera collapse structures have developed in two (Krafla and Askja) of the five spreading segments central volcanoes, reflecting that these are the most mature systems. These are also the only ones to have produced eruptions in historic time (~1000 yr), apart from a briefly

described eruption off the north coast in 1868. The long-term local plate spreading rate is 1.8 cm/yr in the direction N106°E according to the NUVEL-1A model (De Mets et al., 1994) in good agreement with GPS measurements spanning 1993 to 2004 (Árnadóttir et al., in press). According to theory, rifting can be described as a cyclic deformation process consisting of three phases (inter-, co- and post-rifting) with different deformation styles (Sigmundsson, 2006). Inter-rifting periods appear to be characterized by continuous spreading with a velocity in agreement with NUVEL-1A predictions. An inter-rifting period is followed by an active rifting event (co-rifting phase), where dikes are intruded into the upper crust to release extensional strain accumulation from the inter-rifting phase. The co-rifting phase is typically split up in a series of repeated large instantaneous displacements, giving a very high, but short lived spreading velocity in immediate vicinity to the intruded dikes. A co-rifting phase is followed by post-rifting, where the rift-perpendicular deformation rate near the rift axis gradually decrease to the background rate typical for inter-rifting periods (Heki et al., 1993, Hofton and Foulger, 1996a, 1996b; Pollitz and Sacks, 1996). The duration of a post-rifting phase depends on the rheological properties of the materials underlying the recently activated spreading segment. Recent GPS measurements from the Krafla area indicate a relaxation duration of a few decades (Árnadóttir et al., in press).

Our main focus will be on the deformation pattern observed at the Askja segment (Fig. 1). The most recent known rifting episode occurred more than 100 years ago, and this segment is therefore assumed to be in a typical inter-rifting period in the entire time span of our data, whereas our earliest data from the Krafla segment may still be slightly influenced by post-rifting processes (Foulger et al., 1992) in addition to the other deformation sources previously inferred (de Zeeuw-van Dalfsen et al., 2004). The last major rifting episode in the Askja fissure swarm took place in the years 1874–1876 (Sigvaldason et al., 1992). The volcanic activity was mainly focused on the northern part of the fissure swarm, up to a distance of 70 km from the central volcano. However a caldera forming Plinian explosion occurred within the Askja central volcano, creating the most recent caldera structure in the nested complex. Another phase of eruptive activity within the volcanic system occurred in 1921–1929 (Sigvaldason et al., 1992). This however, was a relatively small event which mainly affected the central volcanic complex and a limited section of the southern extent of the fissure swarm. The most recent volcanic eruption at Askja was in 1961, where lava was extruded within the caldera complex. The small magnitude and localized effect of this event, occurring on an east–west striking part of the caldera rim, indicate that it was not a rifting event (Thorarinsson and Sigvaldason, 1962).

2.2. Deformation monitoring and previous modeling

Understanding of divergent plate boundaries has been advanced through various modeling efforts. One set of models has relied on observed crustal deformation fields as a primary constraint, to infer both the processes taking place at extensional rifts as well as their rheological structure. Repeated geodetic measurements spanning periods of eruptive or intrusive activity have been used to derive constraints on magma sources, magma transport and the dimensions of dikes (Tryggvason, 1984). Observations spanning time periods with no eruptive or intrusive activity have been used for studies of rheological structure (e.g. Foulger et al., 1992; Heki et al., 1993; LaFemina et al., 2005; Pagli et al., 2007a).

Crustal deformation has been measured in Iceland for decades, using a range of terrestrial techniques, such as triangulation, electronic distance measurements (EDM), dry-tilt and optical leveling, as well as the space based methods GPS and InSAR. Geodetic measurements of the NVZ were initiated in 1938 with a German triangulation network (Niemczyk, 1943). Direct measurements have captured all phases of the
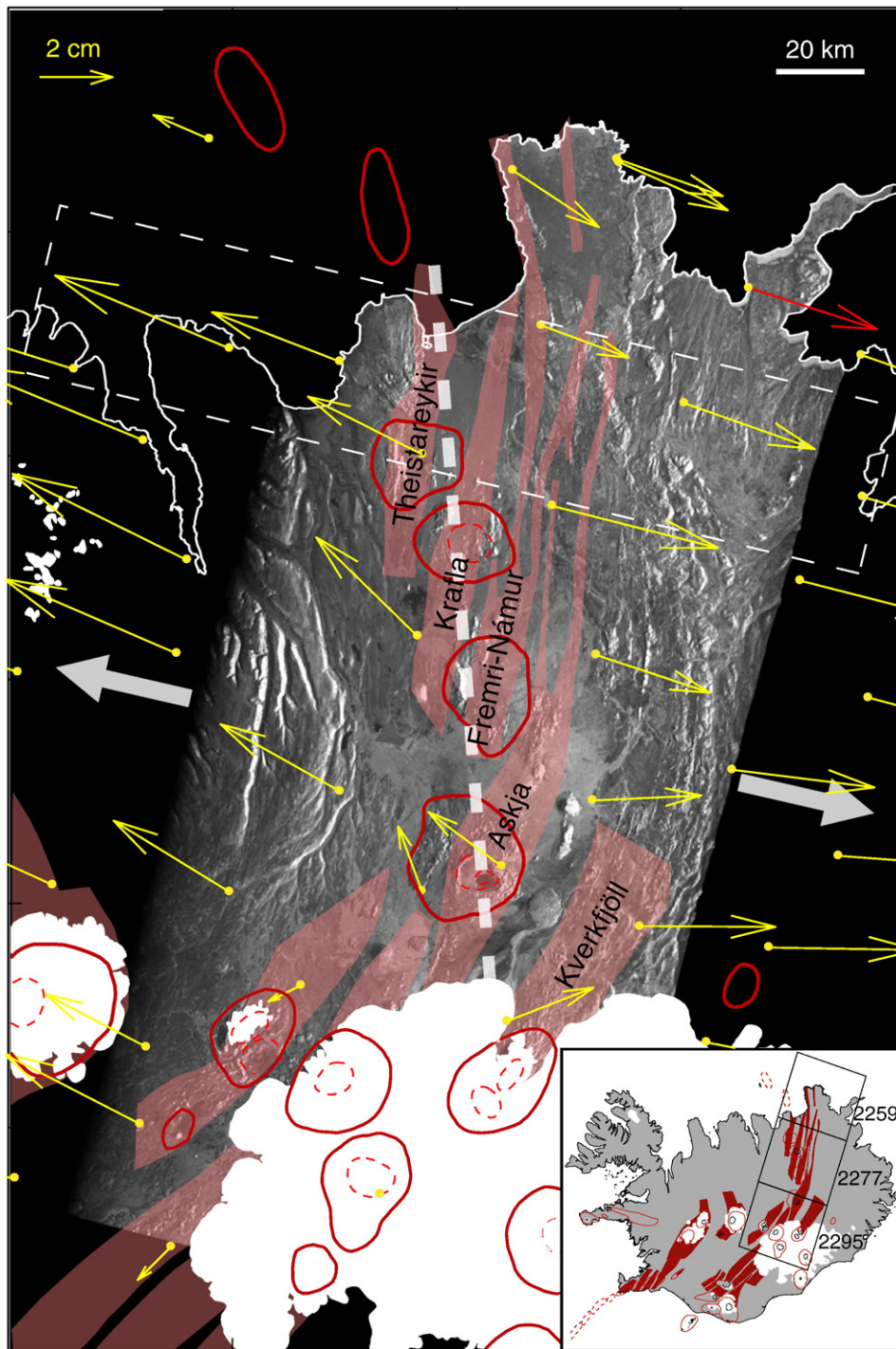
Fig. 1. The Northern Volcanic Zone (NVZ) in Iceland, forming part of the Mid-Atlantic spreading ridge. The thick stippled line illustrates the regional trend of the deformation zone (line through the main centers of magmatic production), oblique to the spreading direction (block arrows). GPS displacement vectors adapted from Árnadóttir et al. (in press) showing 5 years of plate spreading deformation in the NVZ are displayed. The thick (red) GPS vector is used as reference in this illustration. Illustrated study area features are: ellipses — volcanic centers, stippled ellipses — calderas, shaded areas — fissure swarms. White line — coastline; filled white areas — glaciers. The inset shows a map of Iceland with the segmented trend of the spreading ridge illustrated by shaded fissure swarms. The three frames (track 9 of the ERS satellites) utilized in this study are also shown. Tectonics after Einarsson and Sæmundsson (1987). (For interpretation of the references to color in this figure legend, the reader is referred to the web version of this article.)

rifting cycle, though with varying precision of the measurements. Developments in recent years within the field of space geodetic methods have significantly improved the efficiency of making deformation measurements with a high temporal and spatial resolution, creating opportunities for applications of sophisticated deformation models.

GPS-measurements in North Iceland initiated in 1986, after the 1975–1984 Krafla rifting episode, have been utilized as constraints for several different models aimed at exploring rift zone rheology. GPS campaigns were carried out in 1987, 1990, 1992, 1993 and 1995 (Völksen, 2000). Measurements spanning the period 1987–1990 indicated extension rates of up to 5.6 cm/yr or about three times the average spreading rate (Foulger et al., 1992; Jahn, 1992), which can be attributed to transient post-rifting stress relaxation following extensive diking during the 1975–1984 rifting episode. Based on these

initial observations, various models have been invoked to explain the observed post-rifting deformation in Iceland, and the apparent interaction of ductile lower crust with an elastic brittle uppermost crust. These models all simulated horizontal layers of uniform thickness. An initial effort by Foulger et al. (1992) invoked a two-dimensional model with an elastic layer underlain by a Newtonian viscous layer, resting on rigid substratum. Diking, which in this simple model is confined to the elastic layer, leads to the process of subsequent stress diffusion in a post-rifting period, as co-rifting stresses set up in the viscous layer relax over time. An extension of this Newtonian viscosity model by Heki et al. (1993) considered the finite length of dikes and the three-dimensional nature of the problem and provided an improved fit to the GPS-observations. A viscosity of 0.3–2×10^{18} Pa s was inferred for a 5–10 km thick Newtonian viscous layer under an 8–30 km thick elastic layer. This highly variable estimate of the elastic layer thickness may reflect the study's shortcomings in predicting the observed deformation based on regional scale model consisting of horizontal layers of homogenous rheology, whereas we may expect considerable variations in the rheological properties on a regional scale in a rifting environment (Brandsdóttir et al., 1997).

Another class of models includes the viscoelastic nature of material beneath an elastic uppermost layer. One of the models by Hofton and Foulger (1996a,b) is comprised of a uniform elastic layer over a linear (Maxwell) viscoelastic halfspace, with dike injection into the elastic layer. The inferred elastic thickness was 10 km, and the estimated viscosity of the underlying material was 1.1×10^{18} Pa s. A three layer model considering viscoelastic properties was presented by Pollitz and Sacks (1996) to explain the post-rifting GPS displacements in Iceland. They consider a horizontally stratified crust, with individual layers being laterally homogeneous, consisting of an elastic uppermost crust and a viscoelastic lower crust, underlain by a viscoelastic halfspace with different viscosity than the lower crust. Their favored lower crustal viscosity is 3×10^{19} Pa s, and the inferred upper mantle viscosity is about 3×10^{18} Pa s. Today, plate spreading across the NVZ appears to have returned to the steady state spreading velocities characteristic for inter-rifting periods (Árnadóttir et al., in press). In south Iceland, GPS measurements and modeling of the horizontal component of measured inter-rifting deformation have been carried out by Jónsson et al. (1997) and LaFemina et al. (2005).

3. Data

Space geodetic methods have improved spatial and temporal resolution of crustal deformation observations in Iceland. GPS has been utilized since 1986, and was the first technique to conclusively measure extension across the plate boundary zone during inter-rifting periods. GPS studies of the plate boundary deformation have mostly focused on the horizontal component of the motion (Sigmundsson et al., 1995; Jónsson et al., 1997; Hreinsdóttir et al., 2001; LaFemina et al., 2005; Árnadóttir et al., 2006). In this study we use the most recently published regional GPS data (Árnadóttir et al., in press). The typical velocity field shows an increasing rate of spreading away from a central axis to a distance of about 30–50 km from the central axis, where deformation reaches a steady state spreading rate (Fig. 2). Early GPS measurements of vertical deformation have been too sparse and of limited accuracy to show any evident regional pattern of deformation relating to plate spreading processes (Völksen, 2000). However, in the recent study by Árnadóttir et al. (in press) a large scale, regional pattern of uplift due to present day glacial thinning in Iceland has been detected. Local vertical deformation fields related to plate spreading processes are not well resolved spatially, though a general resemblance to our InSAR data exist (Árnadóttir et al., in press, their Fig. 13).

InSAR is another space geodetic technique, which in recent years has provided a wealth of detailed surface deformation measurements (e.g. Massonnet et al., 1994; Pritchard and Simons, 2002; Jónsson et al., 2003; Wright et al., 2004, 2006). Interferograms can be regarded as deformation maps, where each interferometric fringe represents a change in range
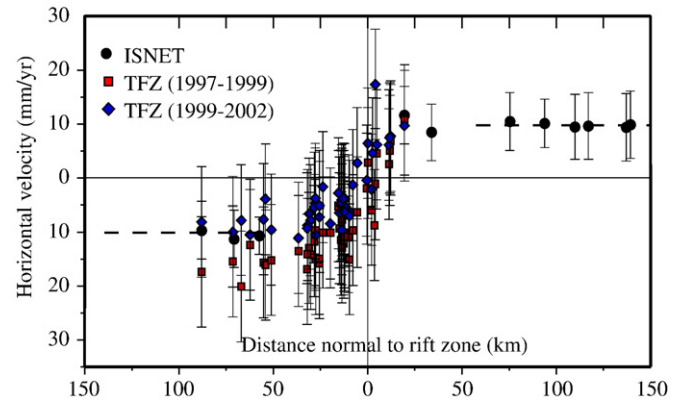

Fig. 2. Horizontal GPS station velocities along a profile in the Krafla area, orientated approximately perpendicular to the direction of the fissure swarms (stippled white box in Fig. 1). The velocities show the spreading across north-east Iceland for the time intervals 1993–2004 (circles), 1997–1999 (squares) and 1999–2002 (diamonds). Profile error bars show the 68% (1σ) confidence interval, and the dashed line is the relative motion predicted by the NUVEL-1A plate motion model. The width of the plate spreading deformation zone is seen to be at least 80 km. The 1993–2004 GPS velocities are from Árnadóttir et al. (in press), while 1997–1999 and 1999–2002 are from Jouanne et al. (2006).

between ground and satellite of 2.83 cm, when data from the ERS-satellites are used (Massonnet and Feigl, 1998). The change in range is measured along the line of sight (LOS) direction. The measurements are therefore one-dimensional, and provide the highest sensitivity to vertical movements, good sensitivity to east–west movements and the least sensitivity to north–south movements, governed by the direction of the unit vector along the satellite LOS. InSAR is therefore ideal for complementing GPS in the NVZ, where only little north–south directed displacement is expected.

A series of InSAR images acquired by the ERS-1 and ERS-2 satellites in the period 1993–2002 have been processed for this study, using the PRISME/DIAPASON software (CNES, 1997) in the two-pass approach (Massonnet and Feigl, 1998). All images were acquired in descending passes, with incidence angles varying from 19 to 27° across each ~100-km-wide scene. Topographic effects have been corrected by use of a digital elevation model (DEM) with a pixelsize of roughly 90 by 90 m, and a vertical precision of about 30 m. All interferograms processed for this study have an altitude of ambiguity (h_a) of 100 m or more and are therefore insensitive to possible small errors in the digital elevation model applied. The h_a is related to the orbital separation between image acquisitions, and equals the size of a DEM error that would produce one artifactual color fringe. Accordingly the InSAR data show the range change associated with crustal deformation and a noise component. We estimate the accuracy of processed InSAR data to be about 1 cm in the LOS direction. Three frames were utilized (from north to south: 2259, 2277, 2295) from a single track (T009) of the ERS satellites (Fig. 1.). We have 17 acquisition dates where all three frames have been stored in the ESA data archive, 6 and 11 additional images in frame 2277 and 2295, respectively. We have formed a total of 19 interferograms from the entire area, an additional 7 covering frames 2277 and 2295, and finally 20 additional interferograms from only frame 2295. An example of a conventional two-pass approach processed interferogram covering the entire area can be seen in Fig. 3. The data span five years (26/06/1993–18/08/1998). Several evident sources of deformation can be recognized. Roughly concentric subsidence areas with locations coinciding with the two central volcanoes, Krafla and Askja, can be seen. These signals are interpreted to be related to deflation of shallow magma chambers as previously described in de Zeeuw-van Dalfsen et al. (2004) and Pagli et al. (2006), respectively. Furthermore, a widespread uplift area is seen to the north of the Krafla volcano, previously suggested by de Zeeuw-van Dalfsen et al. (2004) to be caused by accumulation of magma close to the crust–mantle boundary. Elongated localized deformation fringes closely associated with the Askja, and to
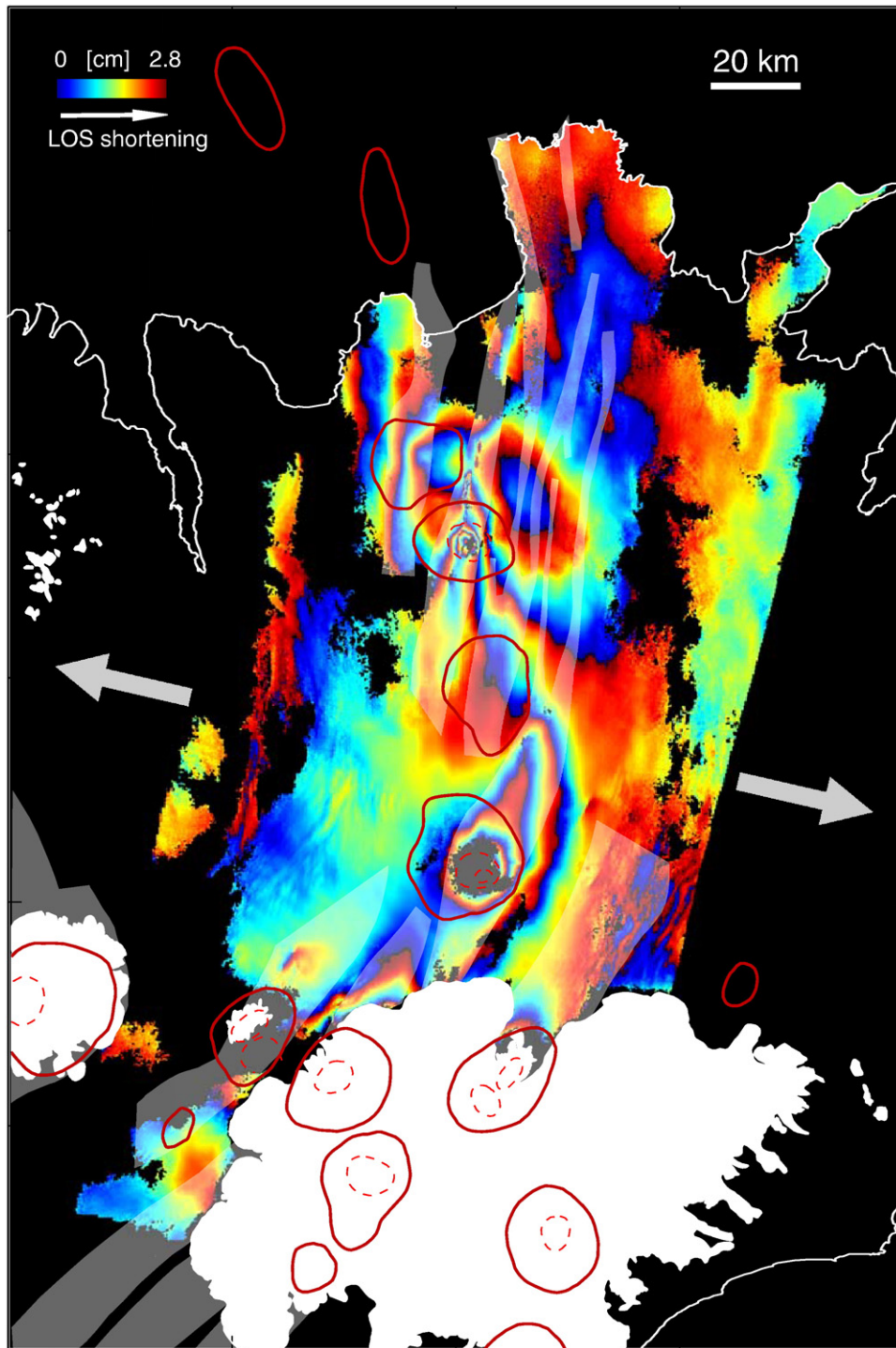
Fig. 3. Conventional interferogram from the NVZ. The SAR data is from track 009; frames 2259, 2277 and 2295; orbits 10174 (ERS1) and 17398 (ERS2). The image is showing 5 years of surface deformation in the plate boundary area — see text for details. An average unit vector for the image is (0.3908, −0.1149, 0.9132) in east, north and up components. The data have been subjected to post-processing plane correction to adjust for inadequate orbital modeling. Tectonics as in Fig. 1.

some extent, the Krafla fissure swarms are evident in the data, but what is equally important is that no such signal is seen associated with the remaining three fissure swarms making up the plate boundary. A slight indication of subsidence is seen at the rim of the glacier, close to the Kverkfjöll central volcano, but no deformation signal is seen to protrude into the fissure segment unlike the deformation in Askja and Krafla (Fig. 3). The signal is not observed in images before 1997. It may relate to the initial stages of a glacial surge from the Dyngjujökull outlet glacier

spanning 1998–1999 (Björnsson et al., 2003). A similar signal at the SW rim of the Vatnajökull icecap has been observed in 1994 and modeling confirms the deformation to be caused by a 20 km³ glacial ice surge (Sigmundsson et al., 2006). The deformation fringes seen on the northwestern rim of the Vatnajökull glacier are due to a subglacial volcanic eruption in the Gjálp system in 1996, which has been investigated by Pagli et al. (2007b). Finally the image is dominated by several north–south striking deformation fringes traversing the entire image. We applied
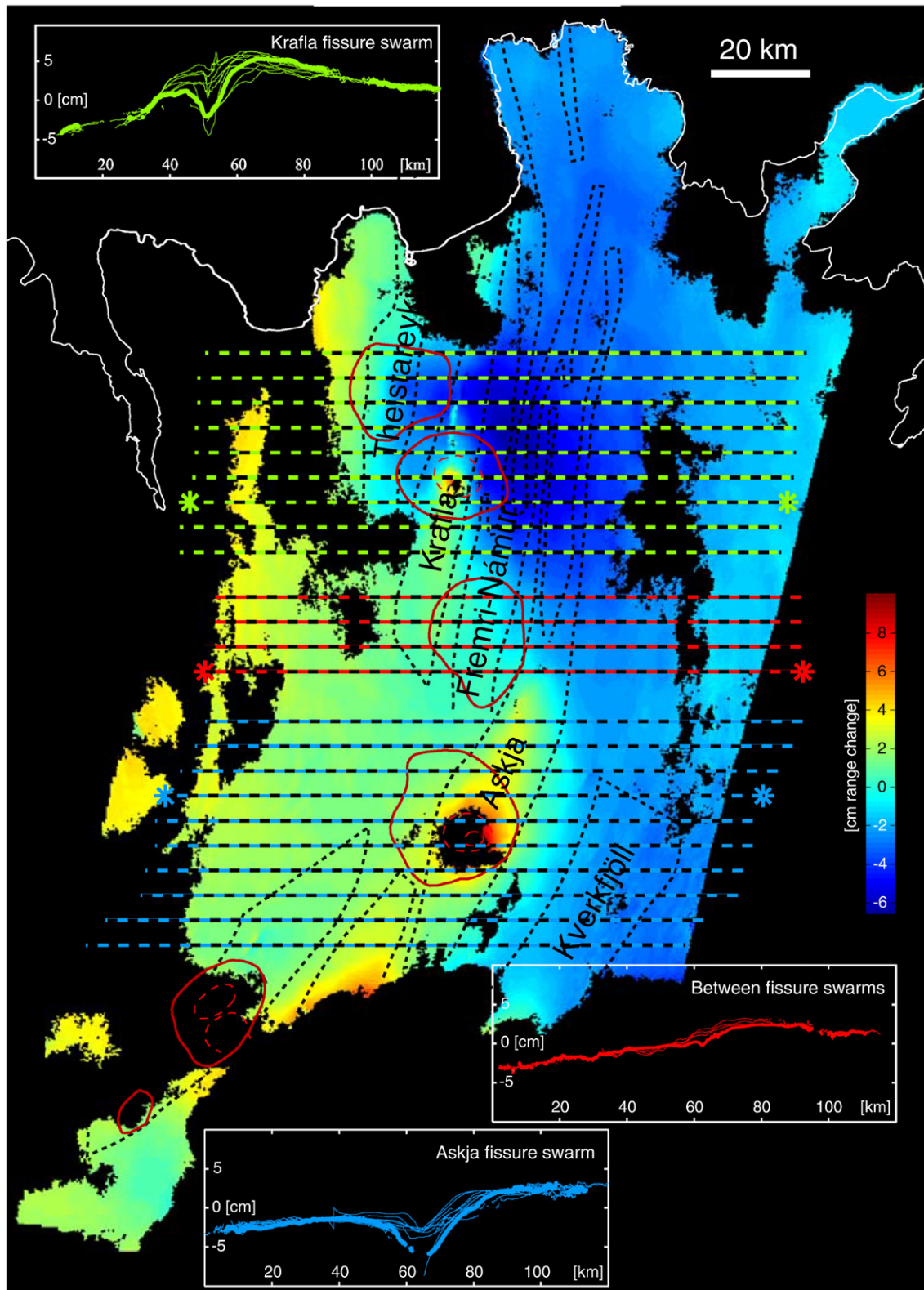
Fig. 4. Unwrapped InSAR data. Negative range change is movement towards the satellite looking from the east. Profiles for three discrete areas are plotted; the Krafla fissure swarm, between fissure swarms, and the Askja fissure swarm. Profiles marked by stars are used as test profiles for the 3D FEM models in Fig. 10, and are plotted with thick lines on the insets. Profiles from the Krafla fissure swarm are projected onto a common center of subsidence. They clearly demonstrate that the area is subjected to a large source of uplift (described and modeled by de Zeeuw-van Dalfsen et al., 2004), partly overprinting the subsidence signal within the fissure swarm as well as the plate spreading signal. The range change profiles from the area between fissure swarms show relatively straightforward plate spreading profiles (gentle slope from east to west), though with a small excess uplift area at the eastern flank, connecting to the broad uplift in the Krafla region. Profiles from the Askja fissure swarm are also projected onto a common center of subsidence. They clearly demonstrate the different length scales of the vertical and horizontal deformation components (gentle slope — horizontal plate spreading signal, bowl shape — fissure swarm subsidence).

post-processing adjustments of the interferometric data to evaluate if part of the north–south striking deformation fringes is caused by insufficient orbital correction, which may add fringes to the image not caused by surface deformation. Because the plate spreading direction and the satellite track is very close to perpendicular, insufficiently precise information of the SAR satellites orbital trajectories may create orbital fringes closely resembling these linear fringes in the resulting interferometric image. This has been considered and corrected. Two locations on each side of the plate deformation zone within the rigid plates were assigned horizontal displacements predicted from the NUVEL-1A plate spreading model and consistent with the GPS measurements. The displacements were projected into the LOS and plotted against the InSAR data to evaluate an appropriate planar data correction to apply. The correction downsizes the initially inferred north–south striking deformation fringes slightly, to the level displayed in the final interferogram shown in Fig. 3. After correction, the magnitude of the north–south striking fringe pattern is consistent with plate spreading and shows a positive correlation with the time span of the data.

In this paper, we do not consider the magmatic deformation sources which all have been described and modeled previously (de Zeeuw-van Dalfsen et al., 2004; Pagli et al., 2006, 2007b). Instead we focus on the surface deformation we infer to be directly associated with plate spreading processes, i.e. the north–south striking deformation fringes as well as the deformation observed within the two fissure swarms at Askja and Krafla. The most interesting and new observation in the series of interferograms compared to existing GPS data in the plate spreading zone, is the difference in length scales between vertical and horizontal deformation components. Vertical deformation seems to be confined within parts of the most recently active mapped fissure swarms, whereas horizontal deformation is distributed over a much broader zone, clearly demonstrated in the three subsets of data profiles in Fig. 4. This decoupling of horizontal and vertical deformation across mapped fissure swarm segments appears to be a basic feature of the plate boundary deformation field that any mechanical model must be able to reproduce.

4. Modeling

The previous studies based on Icelandic deformation measurements, referred to above, mainly focus on modeling post-rifting deformation observed by a network of GPS stations, through lithospheric models that simulate several horizontal, homogeneous rheologic layers. These relatively simple models fail to reproduce the difference in length scales of vertical and horizontal deformation components observed in the geodetic data presented above. Only in the era of space borne geodesy has the combination of high spatial resolution covering large areas, and quality of vertical deformation measurements made detailed mapping of the subtle, widespread vertical adjustments in periods dominated by inter-rifting deformation manageable. This may be one reason why the difference in length scales between horizontal and vertical displacements has not previously been explained by variations in rheology. The interferometric data presented shows that the deformation signal is gradual, almost axisymmetric and coherent within large parts of the fissure swarms, contradicting that the source of deformation may be slight normal faulting close to the surface. We test if the signal can be explained through relatively simple, geologically reasonable rheological variations in the rift forming materials. We investigate the effects of both lateral and vertical variations in rheology and geometry of the lithospheric boundary zone on resulting deformation patterns. FEMs can be used to solve elastic governing equations in arbitrary domain, which is readily partitioned to account for the structural complexity of a volcano complex and rift segment. The FEMs applied in this study are constructed with the general-purpose FEM code Abaqus (http://www.simulia.com). The code solves for displacement (u) over a problem domain having a combination of elastic and viscoelastic

properties. Expressed in index notation, the governing equation for an elastic material is

$$\mu \nabla^2 u_i + \frac{\mu}{(1-2\nu)} \frac{\partial^2 u_k}{\partial x_i \partial x_k} = -F_i \qquad (1)$$

where μ is here the shear modulus, ν is Poisson's ratio and F is a body force (Wang, 2000). Viscoelastic behaviour is simulated by imposing an additional stress-dependent strain-rate relationship on desired regions of the problem domain. The total (viscoelastic) strain rate is the sum of the elastic and creep strain rates. The standard expression for creep strain rate is:

$$\dot{\varepsilon} = A\sigma^n \qquad (2)$$

where $\dot{\varepsilon}$ is the uniaxial equivalent strain rate, A is a constant that can be expanded to include a temperature dependence and thermally activated creep, and σ is deviatoric stress (Carter and Tsenn, 1987). When combined with the elastic strain rate, the relationship is equivalent to a Maxwell material, or linear viscosity law, if $n = 1$ and A is half of the inverse of the linear viscosity. We will use 2D and 3D FEMs to facilitate discrimination between a model where surface deformation due to plate spreading is governed by a central subsurface rift axis and a model where the rheological characteristics of individual fissure swarms play the major role.

4.1. 2D FEM models

Initially, all models have identical outer dimensions (Fig. 5). The width of the model, 50 km, corresponds to the approximate half-width of the strain accumulation zone, as at about 50 km distance from the center of the rift we reach the half-spreading rate of the rigid plate (Fig. 2). In all 2D (plane strain) models we apply identical boundary conditions simulating inter-rifting deformation through plate pull; the models are subjected to no initial stress before the onset of deformation, including no gravity. At the onset of plate pull the model is subjected to stresses resulting in instantaneous strain. Our specific model approach allows us to disregard spin-up of the model by repeated dike-injections,
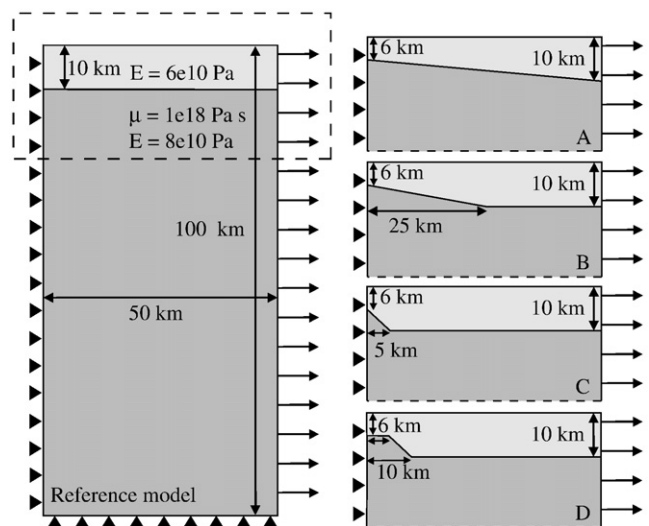

Fig. 5. 2D FEM models for testing the effect on surface deformation of varying layer boundary geometry during inter-rifting periods, simulated by plate pull at the edge of the deformation zone. Rheological parameters are identical for all models and values are stated on the reference model. We use $\nu = 0.25$ for all materials. Black triangles symbolize model boundaries that are kept fixed in the direction of the arrow, but free to move in the perpendicular direction (along model edge). All models have identical dimensions and boundary conditions. A zoom of the upper part of the model is shown for models A to D, corresponding to the stippled box on the reference model. E is the elastic Young's modulus of the material and μ the viscosity.
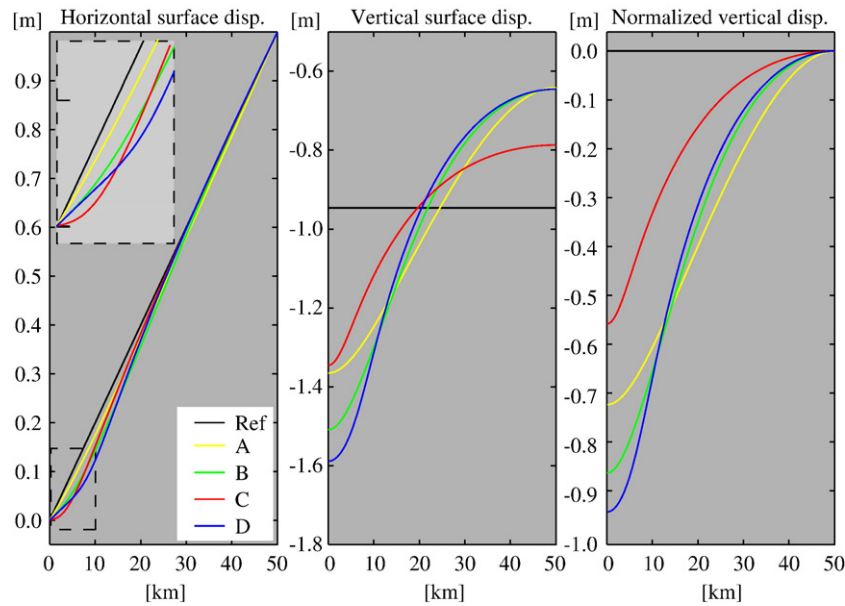
Fig. 6. Horizontal and vertical deformation fields from models in Fig. 5. The left panel shows predicted horizontal displacements at $t = 100$ yr. The center panel shows the absolute vertical surface displacements, and the right panel shows the normalized vertical deformation field, e.g. the vertical displacement of the surface nodes relative to the vertical displacement at the surface node at the far (eastern) edge of the model.

as we apply plate pull as opposed to plate push. Our simple model is used as a crude approximation to the plate spreading environment, where steady state deformation has been reached (inter-rifting stage). Our main aim is to explore the control on surface response within the deforming plate boundary zone exerted by rheological variations in the crustal layers, but not investigate the active rifting processes (co-rifting and post-rifting stages). The left edge, representing the location of the ridge, is pinned with respect to horizontal movements but free to move vertically. The right edge is subjected to plate pulling at a linear rate of 1 cm/yr over a period of 100 years. We do not account for gravitational or isostatic forces, consequently the upper edge represents a free surface with no vertical displacement boundary condition, whereas the lower edge is pinned vertically, but free to move horizontally (Fig. 5).

Our reference model is similar to models proposed previously by others (Foulger et al., 1992; Heki et al., 1993; Hofton and Foulger, 1996a,b). It consists of two horizontal homogeneous layers; a viscoelastic lower layer, representing the ductile lower crust and upper mantle, overlain by a purely elastic layer, representing the upper crust (Fig. 5). All rheological parameters have been chosen within bounds of realistic values for the environment under investigation, but no attempts of precise parameter evaluation or estimation have been made, as such is beyond the scope of this paper. Furthermore, a previous 2D FEM study by Karlsson (2008) investigated surface deformation responses caused by variations of the rheological model parameters (viscosity range investigated: 1×10^{18} Pa s to 1×10^{20} Pa s). The study concluded that the parameter with the least influence on surface deformation is the viscosity of the viscoelastic layer (Karlsson, 2008).

First, we investigate what happens when the geometry of the boundary between the elastic and viscoelastic layer is not horizontal. When the elastic crust thickens gradually away from the ridge, as would be expected from a simple cooling model, a dramatic effect on the resulting surface deformation is seen (model A in Figs. 5 and 6). Where the reference model predicts uniform subsidence over the entire model, a sloping boundary between elastic and viscoelastic layers induces increased subsidence near the rift and less subsidence at the far edge of the model. Increased steepness of the ramp between the elastic and viscoelastic materials produces a limited effect on the horizontal displacements (models B and C in Figs. 5 and 6). However, a steeper ramp induces a narrowing of the area of main subsidence. The key development from models A to C is, that by increasing the steepness of

the ramp, thereby effectively decreasing the volume of the viscoelastic material, horizontal displacements are suppressed in the immediate vicinity of the rift in favor of strong vertical deformation (Fig. 6). In model D we introduce a slightly more complicated rift structure, with thin elastic crust in a broad region in vicinity of the rift, and a relatively steep ramp to thicker elastic crust (Fig. 5). This slightly more complicated rift structure produces an even stronger subsidence bowl near the rift and increases the horizontal deformation in the near rift environment slightly (Fig. 6). These final model complications may not be justified by the resulting deformation field as the model does not contribute any significant new information, but the geometry seems more realistic for a real rift zone.

Next we introduce more rheological variability in the rift zone and use Model C for reference. A wedge of weak elastic material is inserted into the rift, representing highly fractured crust which may be expected in this area (Fig. 7, model C1). Though all rocks in Iceland are
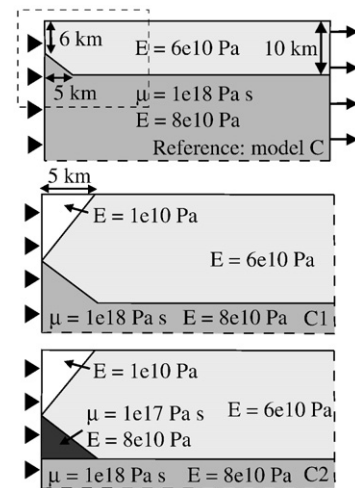

Fig. 7. 2D models for testing the effect on surface deformation of varying rheology during an inter-rifting period. We use model C from Fig. 5 as a reference model. Dimensions and boundary conditions are identical to the previous models. Rheological parameters are here shown on the models. We again use $\sigma = 0.25$ for all materials. The stippled box on the reference model corresponds to the zoom area for model C1 and C2.

essentially produced at the rift zones, we may expect an increase in the rock strength of the upper crustal rocks with increasing age (and thereby distance from the production center (fissure swarm)), facilitated by secondary minerals in fractures and vesicles deposited by circulating geothermal waters (Saemundsson, 1986). The weak elastic wedge has a major influence on both deformation components. Horizontal deformation is strong in the immediate vicinity of the rift (within the area of the weaker material), and tapers to a lower deformation gradient in the remaining elastic crust (Fig. 8). The effect on the vertical deformation component is an even stronger focusing of the deformation into the rift zone.

In the final rheological model presented here, we lower the viscosity of the viscoelastic wedge in the rift zone (Fig. 7, model C2). The low viscosity region may represent an anomaly in the tempera-ture and/or pressure of the region below the weak elastic wedge. The resulting deformation pattern is similar to the previous model, though with a slight increase in both extent and magnitude of the imposed subsidence (Fig. 8).

Models with variable thickness of the elastic upper crust (models A to D) create horizontal displacements fields relatively similar, to the reference model (uniform thickness model), with subtle but distinct deviations in the near rift area (Fig. 6). On the other hand, vertical displacement fields show strong dependence on the slope angle of the rheological boundary and the relative volumes involved. By introdu-cing a wedge of weak elastic material in the rift zone (Fig. 7) we strongly focus both displacement components towards the near rift environment, with maximum effect on the vertical displacement component (Fig. 8). When comparing the results from our 2D reference model to the deformation data it is evident that a horizontal layered, uniform thickness model is inadequate for modeling of plate spreading behaviour, because it fails to reproduce the variations in the vertical displacement component observed in deformation measure-ments. With the introduction of quite simple rheological structures in the near rift environment it is possible to reproduce the main characteristics of both the horizontal and vertical deformation components. InSAR measurements support a model including a weak elastic wedge within the fissure swarms. Additional GPS profiles, with closely spaced measuring points across the fissure swarms, would assist discrimination between models.

4.2. 3D FEM models

So far we have only been looking at the deformational response to plate spreading within a cross section of a single fissure swarm. However the plate boundary in northern Iceland is divided into an *en echelon* arrangement of five fissure swarms. Three dimensional modeling efforts are therefore needed to investigate the interplay between individual fissure swarms thereby addressing the question of what sub-surface feature controls the surface deformation at exten-sional rifts. Based on our 2D model experiments we select appropriate rift rheology models to represent the most recently active fissure swarms, Krafla and Askja. The rift rheology within the remaining three fissure swarms is assumed to be similar to the surrounding crust, with no lateral or vertical variations in rheological parameters. We then construct a 3D model roughly corresponding to the geometry of the NVZ, and investigate the surface deformation field for three different 3D models.

All 3D models have identical outer dimensions, being 100 km east–west, 300 km north–south and extending to 100 km depth (Fig. 9). Our 3D model base is constructed from two *en echelon* fissure swarms. The Krafla fissure swarm is 80 km long, 12 km wide at the surface and strikes N10°E, whereas the Askja fissure swarm is 60 km long, 18 km wide at the surface and strikes N20°E (Fig. 9). We apply boundary conditions simulating inter-rifting deformation through plate pull as for the 2D models. The pull is exerted at the north–south striking boundaries in a oblique direction consistent with the NUVEL-1A model. This causes the width of the strain accumulation zone to be slightly asymmetrical about the center of the fissure swarms. As the exact extent of the plate deformation zone is not well known, we allow this oversimplification for easing model construction. Our 3D models are only crude approximations towards the creation of more realistic plate boundary models of the future, which will ultimately account for the wide variety of complexities known to exist in such an area.

In our first model (Fig. 9, 3DA) the rheological profile of model D (Fig. 5) is extended into 3D and applied to both fissure swarms, i.e. we insert a viscoelastic flat-top wedge extending from 10 km depth at the edge of each of the fissure swarms, reaching to 6 km depth over a distance of 5 km horizontally, resulting in a central horizontal
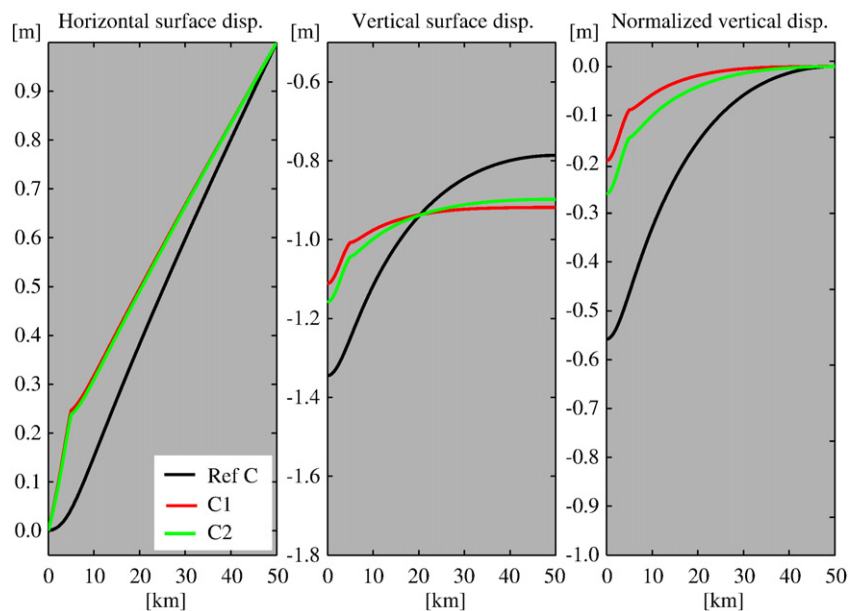

Fig. 8. Horizontal and vertical deformation fields from models displayed in Fig. 7. The left panel shows predicted horizontal displacements at $t = 100$ yr. The center panel shows the absolute vertical surface displacements, and the right panel shows the normalized vertical deformation field, e.g. the vertical displacement of the surface nodes relative to the vertical displacement at the surface node at the far (eastern) edge of the model.
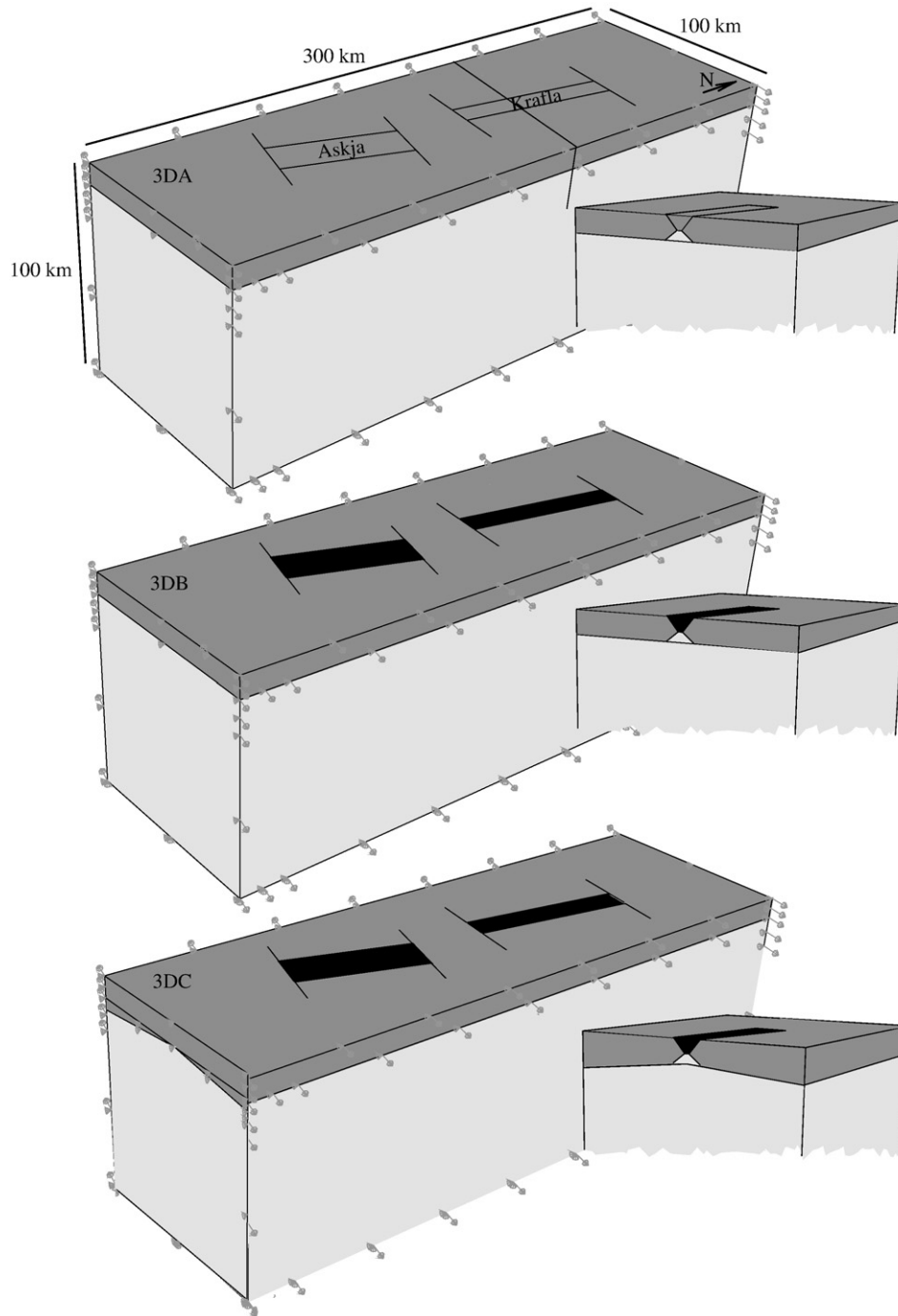
Fig. 9. 3D model sketches. Light grey, grey, and black regions represent visco-elastic, elastic, and weak elastic materials respectively. Rheological parameters as in Model C1 (Fig. 7). Arrow symbols denote boundary conditions. Each model comprises more than 500,000 elements.

boundary of 2 and 8 km for the Krafla and Askja fissure swarms, respectively, in an otherwise horizontally layered model. The resultant surface deformation is projected into the LOS direction (Fig. 10, 3DA) for easy comparison to the unwrapped InSAR data (Fig. 4). Furthermore, model predictions, data and residuals for three selected test profiles are displayed on the figure. RMS values can be found in Table 1. Model 3DA does a fair job in recreating subsidence within the fissure swarms, but the subsidence is too smooth and wide spread when compared to the actual data. The Krafla data profile has a complex deformation signal, where the widespread uplift area previously described is superimposed on the more limited fissure swarm subsidence, which is however evident. Model predictions at

the profile in between fissure swarms show a reasonable fit to the data.

Model 3DB is identical with 3DA except for the introduction of an upper wedge of weak elastic material within the fissure swarm (Fig. 9), in a similar manner as displayed in Fig. 7 (model C1), extending from 6 km depth to the surface. The profiles of resultant surface deformation bears a strong resemblance to the plate deformation signal in the InSAR image (Fig. 10, 3DB). A widespread signal is seen across the entire model due to the plate pull at the edges, but a distinct deformation signal is also apparent within the fissure swarms, as seen in the data. The profile in between fissure swarms shows a slightly improved fit to the data compared to model 3DA.
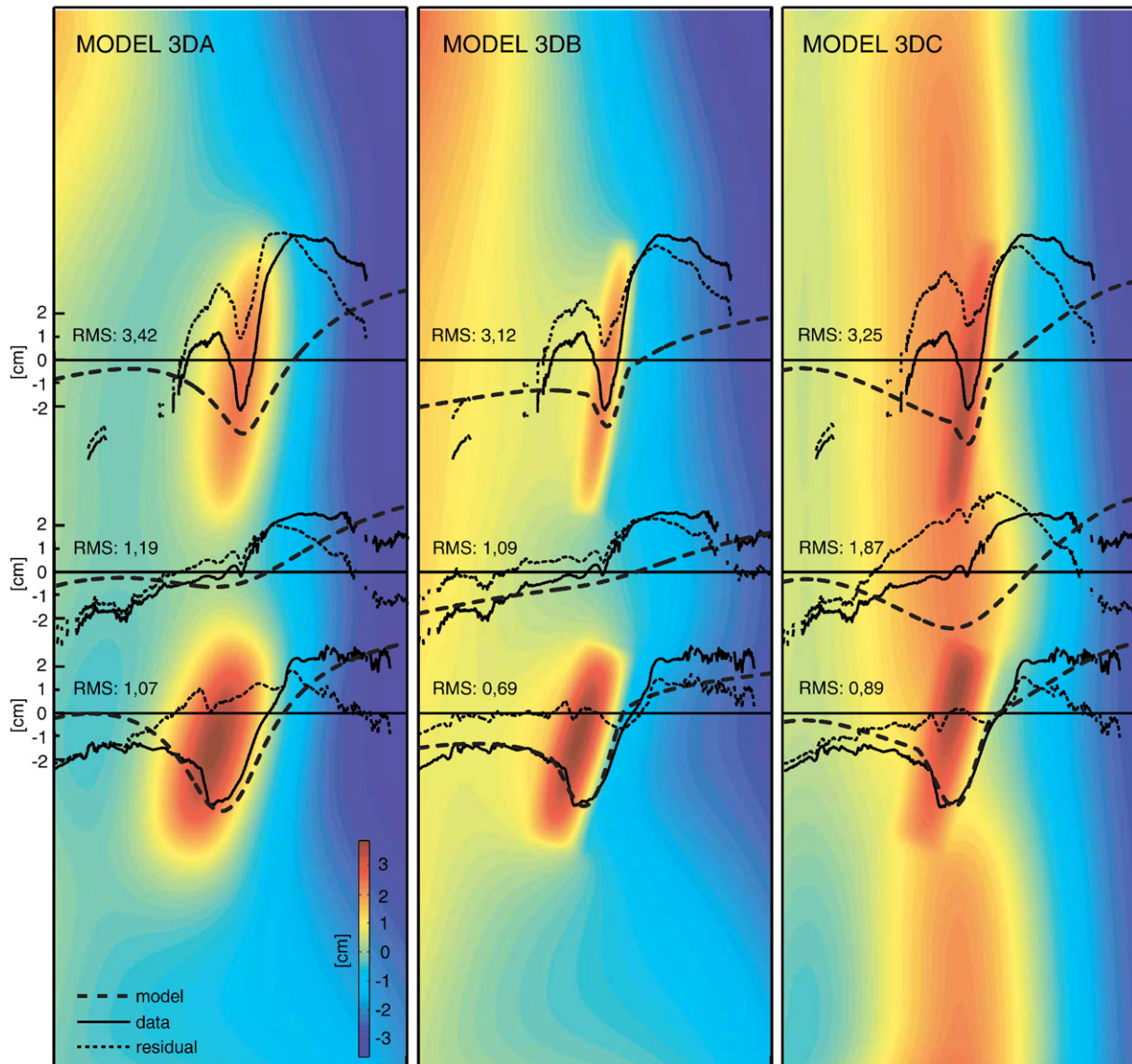
Fig. 10. Predicted map of surface deformation projected into the LOS direction of the SAR satellite of an area corresponding to the surface (map view) of our 3D models. The three black straight lines across the deformation maps show the locations of selected test profiles, which are plotted across the Krafla and Askja fissure swarms, as well as between fissure swarms. Test profile locations of the data are shown in Fig. 4. The location lines are used as baseline (zero), for the profiles displaying the LOS displacements for a 5 year period (thin solid line), model predicted LOS surface displacement for a corresponding duration (thick broken line), and finally model residuals (thin dotted line). For each of the residual profiles the corresponding RMS value is displayed.

In our final model we retain the rheological complexities of the fissure swarms from previously and introduce a central ridge axis beneath the entire model (Fig. 9, model C), to explore the effects of a plate cooling model. The thickness of the elastic plate increases linearly with distance from the central axis. For simplicity, the ridge is implemented with strike N0°E. A wide subsidence area dominates the resultant deformation (Fig. 10, 3DC), especially evident in the profile between fissure swarms, demonstrating that a model where elastic

thickness increases away from the central rift axis does not govern the style of deformation observed in inter-rifting periods.

5. Discussion

Simple crustal models with horizontal layers of uniform thickness may in many cases be sufficient to obtain satisfactory model predictions. However, such models are poor representations of Earth's complexities. Models for cooling of the oceanic lithosphere after time of formation at ridge crests suggest strong variation in rheology next to the ridge axes, and similarly do seismic studies of ridges indicate structural variations. In north Iceland, large variations in the compressional velocity in two dimensions have been inferred from seismic refraction profiles across the plate boundary (Brandsdóttir et al., 1997), hence large variations in the rheology of the crustal rocks with both depth and distance from the center of spreading. Lateral variations in rheology are a fundamental part of plate extension environments, but are often ignored for simplicity during modeling of surface deformation. Recent and future improvements in data

Table 1
RMS values for data profiles (null models; see Fig. 4 for profile locations) and corresponding residuals for the 3D models.

	Krafla fissure swarm (cm)	Between fissure swarms (cm)	Askja fissure swarm (cm)
InSAR data	3.6	1.6	2.2
Model 3DA	3.4	1.2	1.1
Model 3DB	3.1	1.1	0.7
Model 3DC	3.3	1.9	0.9

quantity and quality require more sophisticated deformation models, because the variation in model predictions associated with standard model simplifications can be substantially greater than data uncertainties (Masterlark, 2007). We have shown that by imposing relatively simple but significant adjustments to the geometry of the crustal layers in the near rift environment, it is possible to explain the deformation data here reported, and thereby advance one step further towards creating realistic rheological scenarios for plate spreading zones. The models tested here are simple, but demonstrate clearly how the structure and rheology of the rift zone may affect patterns of surface deformation.

Our FEM modeling is conducted with a closed system assumption. The lower boundary of the model is assumed fixed, with no material flux through it. This causes overall subsidence of the model crust (e.g. Fig. 8, center panel), but the normalized subsidence (e.g. Fig. 8, right panel) mimics our observations. In reality, upward flow of material at the ridge axis can be anticipated as mantle upwelling occurs beneath ridges. Thinning of the uppermost crust by stretching can also lead to isostatic adjustment. The uppermost crust is less dense than the mantle, so crustal thinning will cause uplift in order to ensure isostatic balance at depth. These effects contribute to upward movement of solid material at the base of our models. We therefore consider normalized subsidence as a first order description of anticipated vertical movements at spreading plate boundaries. Future reconfigurations of our models may allow a minimum estimate of upward flow at the ridge axes. Part of this flux may take place by episodic magma transport from mantle to lower crust. Such deep intrusion of magma is inferred from recent seismic and geodetic data to be currently active in the rift zone east of Askja (Geirsson et al., 2008).

Subsidence related to the Askja and Krafla fissure swarms in northern Iceland are apparent in InSAR images from Northern Iceland, together with magmatic deformation sources (Figs. 3 and 4). No similar subsidence is observed in the other three fissure swarms making up the plate boundary zone. It could be argued that the subsidence may origin from aseismic dike intrusions occurring in the fissure swarms. However, we consider this scenario highly unlikely due to the following reasons: 1) Seismicity was consistently seen to be associated with shallow dike intrusions during the Krafla rifting episode (1975–1984); 2) No associated flank uplift have been detected as would be expected from a shallow dike intrusion; 3) No accelerated horizontal deformation has been seen in the flank areas, as would also be expected from a shallow dike intrusion, and 4) We find it unlikely that contemporary aseismic dike intrusions occur within the Krafla and Askja fissure swarms.

The Krafla and Askja volcanic systems have been active in preceding centuries, with the Krafla rifting episode in 1975–1984 and a rifting episode at Askja in 1874–1876. They are the only fissure swarms in the area to have central volcanoes with calderas, indicating that these segments are more mature than the three others, and may therefore have experienced a higher number of rifting events. It has been confirmed that the Krafla fissure swarm has been subjected to at least 6 major rifting events during the past 3000 years (Sæmundsson, 1991). This correlation of fissure swarm subsidence and activity in preceding centuries or millennia (confirmed for Krafla) suggests a link between past magmatic activity and present day fissure swarm subsidence. Our modeling indicates that viscoelastic rheology may reach a shallower depth within these fissure swarms, causing a local thinning of the elastic crust. Such a rheological structure is consistent with the effect of past centuries or millennia of magma intrusions and diking events, supplying additional heat to the most active fissure swarms. As these fissure swarms provide an effective weakness in the crust, they may furthermore be the preferred locus of future activity in the Northern Volcanic Zone.

Our observations can be compared to observations from other parts of the plate boundary in Iceland. Simpler deformation fields than in northern Iceland, similar to our 2D model predictions, are anticipated if a fissure swarm is aligned with the direction of the rift zone. This is the case in the Thingvellir fissure swarm north of the Hengill central volcano in south Iceland, as it is sub-parallel to the western volcanic zone. A modeling approach in two dimensions appears to be capable of explaining subsidence of about 1–4 mm/yr of a central part of the fissure swarm relative to its edges (Tryggvason, 1974; Karlsson, 2008). Our observation of recent fissure swarm subsidence relating to major rifting episodes in prior centuries or millennia suggests, that localized subsidence at fissure swarms may eventually decay with time since the prior rifting episode. Such behavior is consistent with observations from the Reykjanes Peninsula (e.g., Vadon and Sigmundsson, 1997), where subsidence appears to be dominated by a central rift axis but not localized along fissure swarms. The most recent diking episodes in these fissure swarms occurred more than 700 years ago. This length of time may be sufficient to "switch off" or reduce rheological variations in relation to fissure swarms, indicating that not only is the rheology highly variable in space, but may also be a transient feature.

Our models suggests that further improved geodetic data from the Northern Volcanic Zone of Iceland, with at least several closely spaced GPS profiles across the entire plate boundary zone combined with InSAR data from both de- and ascending satellite tracks, hold the potential to reveal further details about the dynamics of volcanic systems arranged *en echelon* at oblique plate boundaries. With more geodetic data at hand, inversion can be attempted to reveal the rheological structure, rather than evaluation of selected forward models. Based on our observations and modeling the following "guide" to deformation in north Iceland emerges (which may be tested in future studies): (1) fissure swarms, where major rifting has occurred in preceding centuries, are weak zones in the plate boundary structure which focus crustal subsidence. (2) The elastic thickness increases away from the individual fissure swarm axes, but not the ridge axis as a whole. (3) For oblique spreading zones, where the fissure swarms are arranged in an *en echelon* pattern along the plate boundary zone, corresponding *en echelon* arranged lateral variations in rheology under the "high-activity" fissure swarms are anticipated to have a major influence on crustal deformation fields.

6. Conclusions

Two dimensional finite element models, consisting of an upper elastic layer and a lower Maxwell viscoelastic layer, subjected to stretching show that topography of the elastic–viscoelastic boundary has a profound influence on the resulting surface deformation field. Induced subsidence focuses towards a rift axis with increasing slope of the elastic–viscoelastic boundary. A smaller, but equally important effect appears when the rheological properties assigned to the crust forming materials are modified, creating a simple way to induce variable length scales for the horizontal and vertical deformation components observed in deformation data. Comparison of FEM model results to InSAR observations in North Iceland require a three-dimensional approach, as fissure swarms of finite width and length are there arranged in an *en echelon* manner. Testing of various geometries for the topography of the elastic–viscoelastic boundary in a rift zone configuration reveals that subsidence in North Iceland can not be attributed to a weakness associated with a central rift axis; rather the crust of distinct fissure swarms active within the past few centuries appear to be weaker than the surroundings. A thin, weak elastic layer overlying a local ridge of viscoelastic material is found to be a likely rheological model for these fissure swarms.

References

Árnadóttir, T., Jiang, W., Feigl, K.L., Geirsson, H., Sturkell, E., 2006. Kinematic models of plate boundary deformation in southwest Iceland derived from GPS observations. J. Geophys. Res 111 (B07402). doi:10.1029/2005JB003907.

Árnadóttir, Th., Lund, B., Jiang, W., Geirsson, H., Einarsson, P., Sigurdsson, T., in press. Glacial rebound and plate spreading: results from the first countrywide GPS observations in Iceland, Geophys. J. Int. doi:10.1111/j.1365-246X.2008.04059x.

Björnsson, H., Pálsson, F., Sigurdsson, O., Flowers, G.E., 2003. Surges of glaciers in Iceland. Ann. Glaciol. 36, 82–90.

Brandsdóttir, B., Menke, W., Einarsson, P., White, R.S., Staples, R.K., 1997. Faroe-Iceland Ridge Experiment. 2. Crustal structure of the Krafla central volcano. J. Geophys. Res 102 (B4), 7867–7886.

Carter, N.L., Tsenn, M.C., 1987. Flow properties of continental lithosphere. Tectonophysics 136, 27–63.

Cattin, R., Doubre, C., de Chabalier, J.-B., King, G., Vigny, C., Avouac, J.-P., Guegg, J.-C., 2005. Numerical modelling of quaternary deformation and post-rifting displacement in the Asal–Ghoubbet rift (Djibouti, Africa). Earth Planet. Sci. Lett. 239, 352–367.

C.N.E.S., 1997. DIAPASON/PRISME Software. France, Toulouse.

De Mets, C., Gordon, R.G., Argus, D.F., Stein, S., 1994. Effect of recent revisions to the geomagnetic reversal time scale on estimates of current plate motions. Geophys. Res. Lett. 21, 2191–2194.

de Zeeuw-van Dalfsen, E., Pedersen, R., Sigmundsson, F., Pagli, C., 2004. Satellite radar interferometry 1993–1999 suggests deep accumulation of magma near the crust–mantle boundary at the Krafla volcanic system, Iceland. Geophys. Res. Lett. 31 (L13611). doi:10.1029/2004GL020059.

Dietz, R.S., 1961. Continent and ocean basin evolution by spreading of the sea floor. Nature 190, 854–857.

Einarsson, P., 1991. Earthquakes and present-day tectonism in Iceland. Tectonophysics 189, 261–279.

Einarsson, P., Sæmundsson, K., 1987. Earthquake epicenters 1982–1985 and volcanic systems of Iceland (map), in: Í. Hlutarsins Eðli: Festschrift for Thorbjörn Sigurgeirsson, Menningarsjóður, Reykjavík Iceland.

Foulger, G.R., 2006. Older crust underlies Iceland. Geophys. J. Int. 165, 672–676.

Foulger, G.R., Jahn, C.H., Seeber, G., Einarsson, P., Julian, B.R., Heki, K., 1992. Post-rifting stress relaxation at the divergent plate boundary in Northeast Iceland. Nature 358, 488–490.

Geirsson, H., Sigmundsson, F., Ófeigsson, B.G., Sturkell, E., Árnadóttir, Th., Hooper, A., Einarsson, P., Guðmundsson, G.B., Jackson, M., Bloom, F., 2008. Crustal deformation associated with the deep-seated seismic swarm at Upptyppingar, north of Vatnajökull, Iceland. IAVCEI General Assembly, Reykjavik, Iceland.

Heki, K., Foulger, G.R., Julian, B.R., Jahn, C.H., 1993. Plate dynamics near divergent boundaries: geophysical implications of post-rifting crustal deformation in NE Iceland. J. Geophys. Res. 98 (B8), 14279–14297.

Hofton, M.A., Foulger, G.R., 1996a. Postrifting anelastic deformation around the spreading plate boundary, north Iceland. 1. Modeling of the 1987–1992 deformation field using a viscoelastic Earth structure. J. Geophys. Res 101 (B11), 25403–25421.

Hofton, M.A., Foulger, G.R., 1996b. Postrifting anelastic deformation around the spreading plate boundary, north Iceland. 2. Implications of the model derived from the 1987–1992 deformation field. J. Geophys. Res. 101 (B11), 25423–25436.

Hreinsdóttir, S., Einarsson, P., Sigmundsson, F., 2001. Crustal deformation at the oblique spreading Reykjanes Peninsula, SW Iceland: GPS measurements from 1993 to 1998. J. Geophys. Res. 106 (13), 803–13,816.

Ito, G., Shenb, Y., Hirth, G., Wolfe, C.J., 1999. Mantle flow, melting, and dehydration of the Iceland mantle plume. Earth Planet. Sci. Lett. 165 (1), 81–96.

Ito, G., Lin, J., Graham, D., 2003. Observational and theoretical studies of the dynamics of mantle plume–mid-ocean ridge interaction. Rev. Geophys. 41 (4), 1017. doi:10.1029/2002RG000117.

Jahn, C.-H., 1992. Untersuchungen über den Einsatz des Global Positioning Systems (GPS) zumNachweis rezenter Erdkrustenbewegungen im Spaltengebiet Nordost-Islands. Ph.D. thesis, WissenschaftlicheArbeiten der Fachrichtung Vermessungswesen der Universität Hannover, Nr. 182, Hannover, Germany.

Jónsson, S., Einarsson, P., Sigmundsson, F., 1997. Extension across a divergent plate boundary, the Eastern Volcanic Rift Zone, south Iceland, 1967–1994, observed with GPS and electronic distance measurements. J. Geophys. Res 102 (B6), 11913–11929.

Jónsson, S., Segall, P., Pedersen, R., Björnsson, G., 2003. Post-earthquake ground movements correlated to pore-pressure transients. Nature 424, 179–183.

Jouanne, F., Villemin, T., Berger, A., Henriot, O., 2006. Rift-transform junction in North Iceland: rigid blocks and narrow accommodation zones revealed by GPS 1997–1999–2002. Geophys. J. Int. 167, 1439–1446.

Karlsson, E., 2008. Finite element modeling of Holocene deformation corresponding to Thingvellir graben, Iceland, in relation to spreading rate and rheology. Nordic Volcanological Center, Institute of Earth Sciences. University of Iceland, p. 79. Report 0802.

Kearey, P., Vine, F.J., 1990. Global Tectonics. Blackwell Science, p. 302.

LaFemina, P.C., Dixon, T.H., Malservisi, R., Árnadóttir, Th., Sturkell, E., Sigmundsson, F., Einarsson, P., 2005. Geodetic GPS measurements in south Iceland: strain accumulation and partitioning in a propagating ridge system. J. Geophys. Res. 110 (B11405). doi:10.1029/2005JB003675.

Massonnet, D., Feigl, K., 1998. Radar interferometry and its application to changes in the Earth's surface. Rev. Geophys. 36 (4), 441–500.

Massonnet, D., Feigl, K., Rossi, M., Adragna, F., 1994. Radar interferometric mapping of deformation in the year after the Landers earthquake. Nature 369, 227–230.

Masterlark, T., 2007. Magma intrusion and deformation predictions: sensitivities to the Mogi assumptions. J. Geophys. Res. 112 (B06419). doi:10.1029/2006JB4860.

Masterlark, T., DeMets, C., Wang, H.F., Sánchez, O., Stock, J., 2001. Homogeneous vs. heterogeneous subduction zone models: coseismic and postseismic deformation. Geophys. Res. Lett. 28 (21), 4047–4050.

Morgan, W.J., 1968. Rises, trenches, great faults, and crustal blocks. J. Geophys. Res. 73 (6), 1959–1982.

Niemczyk, O., 1943. In: Wittwer, K. (Ed.), Spalten auf Island. Stuttgart Germany.

Pagli, C., Sigmundsson, F., Árnadóttir, Th., Einarsson, P., Sturkell, E., 2006. Deflation of the Askja volcanic system: constraints on the deformation source from combined inversion of satellite radar interferograms and GPS measurements. J. Volcanol. Geotherm. Res. 152, 97–108. doi:10.1016/j.volgeores.2005.09.014.

Pagli, C., Sigmundsson, F., Lund, B., Sturkell, E., Geirsson, H., Einarsson, P., Árnadóttir, Th., Hreinsdóttir, S., 2007a. Glacio-isostatic deformation around the Vatnajökull ice cap, Iceland, induced by recent climate warming: GPS observations and Finite Element Modeling. J. Geophys. Res. 112 (B08405). doi:10.1029/2006JB004421.

Pagli, C., Sigmundsson, F., Pedersen, R., Einarsson, P., Árnadóttir, Th., Feigl, K.L., 2007b. Crustal deformation associated with the 1996 Gjálp subglacial eruption, Iceland: InSAR studies in affected areas adjacent to the Vatnajökull ice cap. Earth Planet. Sci. Lett. 259 (1–2), 24–33.

Pollitz, F.F., Sacks, I.S., 1996. Viscosity structure beneath northeast Iceland. J. Geophys. Res. 101 (B8), 17771–17793.

Pritchard, M.E., Simons, M., 2002. A satellite geodetic survey of large-scale deformation of volcanic centres in the central Andes. Nature 418, 167–171.

Ruegg, J.C., Briole, P., Feigl, K.L., Orsoni, A., Vigny, C., Anis Abdallah, M., Bellier, O., de Chabalier, J.-B., Huchon, P., Jacques, E., Al Kirbash, S., Laike, A., d'Oreye, N., Prévot, M., 1993. First epoch geodetic GPS measurements across the Afar plate boundary zone. Geophys. Res. Lett. 20 (18), 1899–1902.

Saemundsson, K., 1979. Outline of the geology of Iceland. Jökull 29, 7–28.

Saemundsson, K., 1986. Subaerial volcanism in the western North Atlantic. In: Vogt, P.R., Tucholke, B.E. (Eds.), The Geology of North America, Volume M: The Western North Atlantic Region, 69–86. Geological Society of America, Boulder, CO.

Sigmundsson, F., 2006. Iceland Geodynamics − Crustal Deformation and Divergent Plate Tectonics. Springer, p. 209.

Sigmundsson, F., Einarsson, P., Bilham, R., Sturkell, E., 1995. Rift-transform kinematics in south Iceland: deformation from Global Positioning System measurements, 1986 to 1992. J. Geophys. Res 100 (B4), 6235–6248.

Sigmundsson, F., Pedersen, R., F eigl, K.L., Pinel, V., Björnsson, H., 2006. Elastic Earth response to glacial surges: crustal deformation associated with rapid ice flow and mass redistribution at Icelandic outlet glaciers observed by InSAR. EGU General Assembly, Vienna, Austria. Geophys. Res. Abstr. 8, 07822.

Sigvaldason, G.E., Annertz, K., Nielsson, M., 1992. Effect of glacier loading/deloading on volcanism: postglacial volcanic production rate of the Dyngjufjoll area, central Iceland. Bull. Volcanol. 54, 385–392.

Sæmundsson, K., 1991. Jardfraedi Kröflukerfisins (Geology of the Krafla volcanic system). In: Einarsson, Árni, Gardarsson, Árnthór (Eds.), Náttúra Mývatns. Hid íslenska náttúrufraedifélag, pp. 26–95 (In Icelandic).

Thorarinsson, S., Sigvaldason, G.E., 1962. The eruption in Askja, 1961. A preliminary report. Am. J. Sci. 260, 641–651.

Tryggvason, E., 1974. Vertical crustal movement in Iceland. In: Kristjansson, L. (Ed.), Geodynamics of Iceland and the North Atlantic Area. Reidel Publishing Company, Dordrecht-Holland, pp. 241–262.

Tryggvason, E., 1984. Widening of the Krafla fissure swarm during the 1975–1981 volcano-tectonic episode. Bull. Volc. 47 (1), 47–69.

Vadon, H., Sigmundsson, F., 1997. Crustal deformation from 1992–1995 at the Mid-Atlantic Ridge, SW Iceland, mapped by satellite radar interferometry. Science 275, 193–197.

Vigny, C., de Chabalier, J.B., Ruegg, J.-C., Huchon, P., Feigl, K.L., Cattin, R., Asfaw, L., Kanbari, K., 2007. Twenty-five years of geodetic measurements along the Tadjoura–Asal rift system, Djibouti, East Africa. J. Geophys. Res. 112 (B06410). doi:10.1029/2004JB003230.

Völksen, C., 2000. Die Nutzung von GPS für die Deformationsanalyse in regionalen Netzen am Beispiel Islands, Ph.D. thesis, Wissenschaftliche Arbeiten der Fachrichtung Vermessungswesen der Universität Hannover, Nr. 237, Hannover, Germany.

Wang, H.F., 2000. Theory of Linear Poroelasticity: With Applications to Geomechanics. Princeton University Press, p. 287.

Wilson, J.T., 1965. A new class of faults and their bearing on continental drift. Nature 207, 343–347.

Wright, T.J., Parsons, B., England, P.C., Fielding, E., 2004. InSAR observations of low slip rates on the major faults of western Tibet. Science 305, 236–239.

Wright, T.J., Ebinger, C., Biggs, J., Ayele, A., Yirgu, G., Keir, D., Stork, A., 2006. Magma-maintained rift segmentation at continental rupture in the 2005 Afar dyking episode. Nature 442, 291–294. doi:10.1038/nature04978.